Environ Geol (2005) 47: 1062–1071
DOI 10.1007/s00254-005-1239-9

ORIGINAL ARTICLE

Ching-Pin Tung
Chung-Che Tan

An optimal procedure for identifying parameter structure and application to a confined aquifer

Received: 14 September 2004
Accepted: 12 January 2005
Published online: 30 March 2005

C.-P. Tung (✉) · C.-C. Tan (✉)
Department of Bioenvironmental Systems Engineering, National Taiwan University, Taipei, 106, Taiwan
E-mail: cptung@ntu.edu.tw
E-mail: aliking@sdl.ae.ntu.edu.tw
Tel.: +886-2-23620327
Fax: +886-2-23635854

Abstract This study applies an optimal procedure to identify the spatial distribution of groundwater hydraulic conductivity for a confined aquifer in north Taiwan. The parameter structure is determined by the number of zones, zonation pattern, and an uniform hydraulic conductivity associated with each zone. The proposed optimal procedure uses the Voronoi diagram in describing zonation and applies simulated annealing algorithm to optimize its pattern and associated hydraulic conductivity. Three criteria are defined to stop the searching process, including the residual error, the parameter uncertainty, and the structure error. Observation hydraulic heads in years 2000 and 2001 and hydraulic conductivity value from pumping tests are used. The results show that the parameter structure with five zones conforms to the three criteria and, thus, is recommended for future groundwater simulation for the study site. Different heuristic algorithms may also play the role of simulated annealing to optimize the parameter structure. However, which optimization algorithm is more efficient is not discussed and requires further study.

Keywords Groundwater · Inverse problem · Simulated annealing · Voronoi diagram · Taiwan

Introduction

Groundwater is an important water resource. Reasonable utilization and proper management of groundwater require an assessment of its availability and the related properties. Researchers have been interested in identifying the spatial distribution of the hydraulic conductivity or transmissivity for groundwater models for the last decades (Yeh and Yoon 1981; Yeh 1986; Zheng and Wang 1996; Sophocleous et al. 1999; Abdulla et al. 2000; Lin et al. 2001; Tsai et al. 2003a, 2003b). They used different approaches to calibrate parameters for groundwater models. For example, Yeh and Yoon (1981) and Yeh et al. (1983) applied the finite element interpolation to construct the spatial distribution of transmissivity. Tung and Chou (2002) and Tung et al. (2003) utilize the pattern zonation methods to calculate the transmissivity.

Sun et al. (1998) reported that the parameterization may be restricted by the parameter uncertainty and the model structure error. The spatial distribution of hydraulic conductivity is important for groundwater simulation. Before running the simulation model, the study area is divided into grids. Different interpolation methods can be used to assign parameters for each grid. Hydraulic conductivity assigned correctly to each grid will result in reasonable simulated hydraulic heads, but determination of the parameters for each grid will have too many variables. It may cause difficulty to find a satisfied optimal solution or to find unique and stable optimal solutions, i.e. same initial solution may converge to different final solutions. If the data insufficient, such

as observed hydraulic heads, high uncertainty is what will be involved. Zonation methods can reduce the dimension of parameterization problems, but requires optimization algorithm to identify the promising zonation and its associated hydraulic conductivity in groundwater simulation.

Over-pumping of groundwater from a confined aquifer, the Chingmei Layer, in the north of Taiwan caused land subsidence in the 1950s. The land subsidence has been stopped and the groundwater level has been restored over the original level since a reservoir was built to provide the water supply and groundwater pumping has been prohibited since two severe droughts in 2002 and 2003 provoked the local water authority to reconsider the groundwater as a supplemental water resource. However, it needs to know how groundwater levels will be controlled to avoid reactivation of the land subsidence. Thus, identification of the spatial distribution of hydraulic conductivity for a reasonable head simulation becomes a first task.

A procedure to identify the spatial distribution of hydraulic conductivity is developed and applied to the Chingmei Layer in this study. The Voronoi diagram (VD) (Dirchlet 1850; Voronoi 1908) is used to define the zonation of hydraulic conductivity, and then simulated annealing (SA) algorithm is utilized to optimize the zonation with the objective to minimize the differences between the observed and simulated hydraulic heads. Meanwhile, the zonation method, VD, is initiated with two zones and one zone is added at one time. Parameter uncertainty, PU (Yeh and Yoon 1981), and the structure error, SE (Sun et al. 1998) are used as termination criteria for additional number of zones.

In Materials and methods section, which introduces VD and SA to formulate the optimal procedure. During the optimal procedure, there are three criteria for determining the optimal structure of parameters, and they are the residual error (RE), the PU, and the SE. These criteria are discussed in Structure identification criteria section. The Case study section addresses the application of the optimal procedure to the Chingmei Layer. The conclusions and suggestions are provided in the last section.

Materials and methods

The spatial distribution of hydraulic conductivity is described by several zones and each zone has a uniform hydraulic conductivity in this study. Thus, the optimization procedure needs to determine the number of zones, the zonation pattern, and the values of associated hydraulic conductivities. The flowchart to identify the spatial distribution of hydraulic conductivity is shown in Fig. 1. Initially, two zones and two randomly assigned hydraulic conductivities are given. Then, the zonation pattern is depicted by the VD and optimized by SA. If the procedure does not meet the three termination criteria, the number of zones will be increased gradually. The zonation method, VD, and the optimization algorithm, SA, are briefly introduced here, while the three criteria are addressed in a later section.

Voronoi diagram

The VD was first introduced by mathematicians Dirichlet (1850) and Voronoi (1908), and it has been applied to many fields. For example, the Thiessen method (1911) used the Voronoi diagram in hydrology to define the spatial pattern of precipitation for calculating the areal average rainfall. Tsai et al. (2003a, 2003b) and Tung et al. (2003) have applied the Voronoi diagram to optimize the zonation of hydraulic conductivity. Although VD has been studied more than one and half centuries, it remains a powerful tool for spatial and pattern analysis (Okabe et al. 1992).

In this paper, VD is used as a zonation method and each Voronoi polygon refers to one individual zone which has a uniform hydraulic conductivity. To construct VD, a finite number of points, n, in Euclidean plane are first considered and assumed that $2 \leq n < \infty$. The n points are respectively labeled by $p_1,..., p_n$ with location vectors $\mathbf{x}_1, ..., \mathbf{x}_n$. The n points are distinct in the sense that $\mathbf{x}_i \neq \mathbf{x}_j$ for $i \neq j$, i, j belong to $I_n(1, ..., n)$.

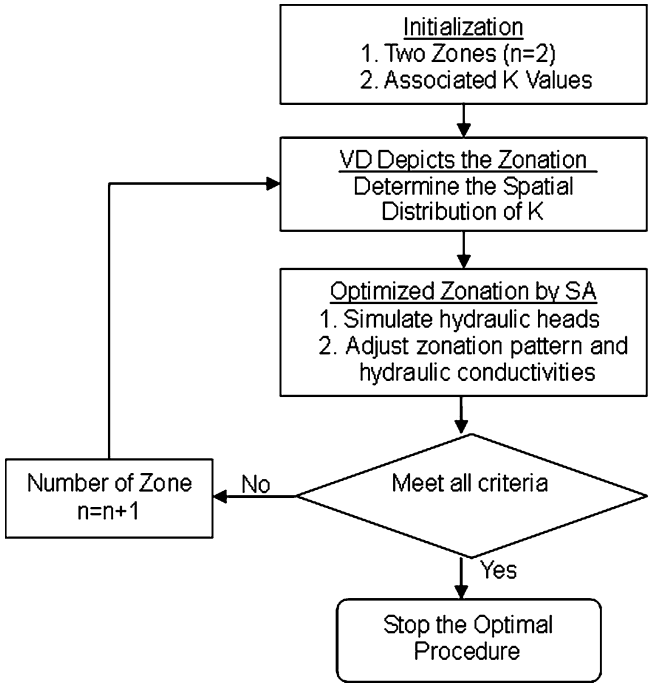

Fig. 1 Flowchart of the optimal procedure

Let p be an arbitrary point in the Euclidean plane with location vector $\mathbf{x}$. Then the Euclidean distance form p to p_i is given by $d(p, p_i) = ||\mathbf{x} - \mathbf{x}_i||$. If p_i is the nearest point from p, i.e. $||\mathbf{x} - \mathbf{x}_i|| \leqslant ||\mathbf{x} - \mathbf{x}_j||$ for all $j \neq i$, p is assigned to the zone $V(p_i)$ containing p_i. Therefore, each Voronoi polygon, $V(p_i)$, can be represented as the following:

$$V(p_i) = \left\{ \mathbf{x} \middle| \|\mathbf{x} - \mathbf{x_i}\| \leqslant \left\|\mathbf{x} - \mathbf{x_j}\right\|, \text{for } j \neq i, j \in I_n \right\} \quad (1)$$

where the Euclidean distance from p to p_i is given by $\|\mathbf{x} - \mathbf{x_i}\| = \sqrt{(\mathbf{x} - \mathbf{x_i})^{\mathrm{T}}(\mathbf{x} - \mathbf{x_i})}$ (which T denotes the transpose operator) and each Voronoi polygon associated with p_i. Then, a plane V can be divided in to a set of Voronoi polygons and is given as Eq. 2.

$$V = \{V(p_1), \ldots, V(p_n)\} \quad (2)$$

where p_i is the generator point of Voronoi polygon $V(p_i)$, and the set $p = \{ p_1, ..., p_n \}$ is called the generator set of VD(V). An example with six generator points is shown in Fig. 2. For the rigorous mathematical properties and applications of VD, readers can refer to Okabe et al. (1992).

Voronoi diagram can partition a domain into several sub-domains after the locations of generator points are determined. The different spatial patterns can be defined by changing the locations of generator points. The best locations of generators to identify spatial distribution of hydraulic conductivity can be optimized by the simulated annealing algorithm.

Simulated annealing

The SA has received much attention in recent years, because it has a mechanism to escape from a local optimum and thus has more chances to reach the global optimum. The basic concept of SA was first introduced by Metropolis et al. (1953). Then, Kirkpatrick et al. (1983) successfully applied the method to combinatorial optimization problems. The optimization procedure of SA is analog to the annealing process of a solid. At high temperatures, all possible states can be reached. Then, the cooling process reduces the number of accessible states and the system is finally frozen in its stable state. As in an optimization process, a system initially has higher probability to accept inferior solutions to explore more alternatives. Gradually, the strategy of intensification dominates the searching process and thus the acceptable probability of inferior solutions becomes less and less. Finally, the search process converges to an optimal state.

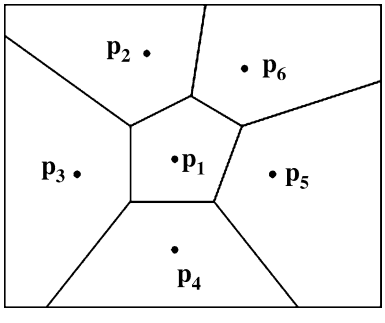

Fig. 2 An example of Voronoi diagram with six zones

The SA adopts the acceptance probability as shown in Eq. 3 to allow moving to the inferior neighbor solution, which brings SA more chances to escape from local optimum and then move toward the global optimum.

$$B_{ij}(\tau) = \begin{cases} \exp\left(-\frac{\Delta C_{ij}}{\tau}\right) & \text{if } \Delta C_{ij} > 0 \\ 1 & \text{if } \Delta C_{ij} \leqslant 0 \end{cases} \quad (3)$$

where B_{ij} is the probability of accepting a move, $\Delta C_{ij} = C_j - C_i$ which C_i and C_j denote the values of objective function of the current and neighboring solutions, respectively. When $\Delta C_{ij} \leq 0$, the neighboring solution is better for minimization problem and the probability to move is equal to 1. On the other hand, when $\Delta C_{ij} > 0$, the neighboring solution is worse and the chance to move is less than one. Besides, the larger C_j, the smaller probability to accept a movement. The inferior solution is accepted only when $\xi \leq B_{ij}$, which ξ is a sampled uniform random number between 0 and 1.

The parameter τ in Eq. 3 is temperature parameter, but it has nothing to do with the real groundwater temperatures. It relates to the cooling schedule which has three parameters: (1) the initial temperature (τ_i), (2) the ending temperature (τ_e), and (3) the decrement (r) in temperature, $0 < r < 1$. Each temperature state has the same searching iteration number L. After L iterations are reached, new temperature (τ) at state $u+1$ is calculated as $\tau_u + 1 = r \times \tau_u$. For more details about how to set the parameters in the cooling schedule can refer to Kirkpatrick (1984), Aarts and van Laarhoven (1985), and Dougherty and Marryott (1991).

Simulated annealing includes four major steps: (a) determine an initial solution and the initial temperature (τ_i) for Eq. 3; (b) randomly sample a solution from the neighborhood of current solution, and then evaluate the value of objective function of the solution; (c) calculate the probability to accept the sampled solution, and generate an uniformly distributed random number to determine whether the sampled solution is accepted; (d) check whether reduction of temperature parameter is required and whether new temperature τ_{u+1} is lower than τ_e to end the searching process. Otherwise, go to step (b).

Structure identification criteria

The VD zonation method is applied to depict the parameter spatial distribution for the groundwater simulation model. A parameter structure relates to its number of zones and can be described by Eq. 4. Different parameter structures represent different parameter spatial distribution.

$$\Omega_n = \mathrm{VD}[V(P_i, k_i), \quad i = 1, \ldots, n] \tag{4}$$

where Ω_n represents the spatial distribution of hydraulic conductivity K with n Voronoi polygons. Each Voronoi polygon is determined by locating the associated generator point and has an assigned attribute of K-value. For example, if n is equal to 2, there are two generator points to determine two zones and each is associated with one hydraulic conductivity. Grids within the same zone have the same K-value. Different numbers and locations of generator points depict different parameter structure Ω_n.

In this study, SA is applied to optimize the location of generator points and associated K-values. Then, the optimal parameter structure Ω_n* is expected to be identified and input to the model to simulate the most accurate hydraulic heads. In the optimal procedure, the number of zones starts with two zones ($n = 2$) and increases one zone at a time until the optimal parameter structure is identified (Tung et al. 2003a, b). The parameter structure with one zone is not considered here. The optimal number of zones n is determined based on three criteria, the RE to minimize simulation error of hydraulic heads, the PU, and the SE.

Residual error

To determine weather, the optimal parameter structure is identified to compare observed information with simulated information. In most cases, the detailed information of a real field is hardly known. There is just some prior information, such as the sited K-values from the pumping tests and the observed hydraulic heads from wells. Therefore, RE can be quantified by Eq. 5.

$$\mathrm{RE}_n = \mathrm{Min}\left\{ \frac{1}{N_h \times T} \sum_{\mu=1}^{N_h} \sum_{t=1}^{T} \left(\frac{h_\mu(\Omega_n, t) - h_\mu^o(t)}{h_\mu^o(t)} \right)^2 + \lambda \frac{1}{N_k} \sum_{v=1}^{N_k} \left(\frac{K_v(\Omega_n) - K_v^{\mathrm{prior}}}{K_v^{\mathrm{prior}}} \right)^2 \right\} \tag{5}$$

where T is the simulation periods; λ is a weighting factor; N_h and N_k are the numbers of observation wells and pumping test well, respectively; RE_n is the minimized residual errors due to parameter structure Ω_n. There are two parts of the RE considered in Eq. 5. The first part is to minimize the difference between the simulated and observed hydraulic heads, and the second is to compare hydraulic conductivities obtained from pumping test with the identified ones by the proposed procedure. In Eq. 5, h_μ and h_μ^o are simulated and observed hydraulic heads for well μ, and K_v and K_v^{prior} are assigned K-based on parameter structure Ω_n and known K from the pumping test for site v, respectively. If there is no prior information of hydraulic conductivity in the study area, λ can be zero.

Parameter uncertainty

The increase in the number of zones and, thus, increase in the parameter dimensions, will result in the decrease in the residual error. However, the parameter structure is becoming more and more complicated. The more unknown parameters need to be determined, the more uncertainty can be expected when prior information is limited. Thus, only using previously described RE to determine the optimal parameter structure is insufficient. A covariance matrix as given by Yeh and Yoon (1981) is adopted to quantify the parameter uncertainty. The trace or the norm of the covariance matrix can be used to compute the parameter uncertainty. Yeh and Yoon (1981) suggested the maximal dimension before a steep raise of parameter uncertainty is recommended as the optimal parameter dimension.

Structure error

Once the number of zones is defined, an optimal parameter structure Ω_n* ($n \geq 2$) can be identified by SA. Theoretically, the global optimum can be reached by SA (Aarts and Van Laarhoven 1985). Thus, the Ω_n* should be analogous to the real case with n approaching the infinite zones. However, the number of n is limited due to parameter uncertainty discussed previously. During the simplifying of the parameter structure, there is a structure error ($\mathrm{SE}_{n,n\text{-}1}$) between two consecutive optimal parameter structures. Sun et al. (1998) proposed three kinds of spaces to illustrate the $\mathrm{SE}_{n,n\text{-}1}$, including the observation space, parameter space, and prediction space.

$$\mathrm{SE}_{n,n-1} = d_{n,n-1}^{\mathrm{obs}}\left(\Omega_n^*, \Omega_{n-1}^*\right) + \omega_1 d_{n,n-1}^{\mathrm{par}}\left(\Omega_n^*, \Omega_{n-1}^*\right) + \omega_2 d_{n,n-1}^{\mathrm{pre}}\left(\Omega_n^*, \Omega_{n-1}^*\right) \tag{6}$$

where ω_1 and ω_2 are weighting factors.

If there is sufficient prior information and observed hydraulic heads, the higher dimension of the optimal parameter structure can be identified to approximate more to the real case. As the result, the trend of $\mathrm{SE}_{n,n\text{-}1}$ between Ω_n^* and Ω_{n-1}^* is going down with the increasing number of zones. However, $\mathrm{SE}_{n,n\text{-}1}$ is analyzed by three

kinds of spaces respectively in this optimal procedure. Then, the optimal parameter structure might be identified by considering the conjunction of the results from three kinds of spaces. A Case study case is discussed in the following section.

A case study

The optimal procedure to identify the spatial distribution of hydraulic conductivity (K) is applied to a confined aquifer, the Chingmei Layer in northern Taiwan. The study area is about 240 km^2 as shown in Fig. 3. The results are also compared with those obtained from traditional gradient method.

Numerical model of the study area

The Processing MODFLOW developed by International Ground Water Model Center (IGWMC) is used in this study. The study area is first divided into 21 columns and 18 rows and the size of each grid is 1×1 km, as shown in Fig. 4. There are total 23 observation wells in this area and Fig. 4 shows the locations of these wells denoted as #1∼#23. Time-variant heads are set as the boundary conditions according to the observed data from ten wells close to the boundaries (#8,#12,#13,#14,#15,#16,#17,#19,#20, and#23).

Moreover, some prior information of hydraulic conductivity for ten drilling wells (*1∼*10) within the basin is used in this study. The locations of these wells are depicted in Fig. 4 and their hydraulic conductivities are listed in Table 1. The values of hydraulic conductivity shown in Table 1 are reported by Water Resources Agency in Taiwan, which are calculated by the Theis groundwater flow equation with data collected from field pumping tests. The specific storage (S_s) is constant and set to be 0.001 referred to a previous study (Hsu 1985). During the last three decades, pumping of groundwater is almost forbidden in this area and thus is omitted during the simulation. In addition recharge to the confined aquifer is assumed to be negligible.

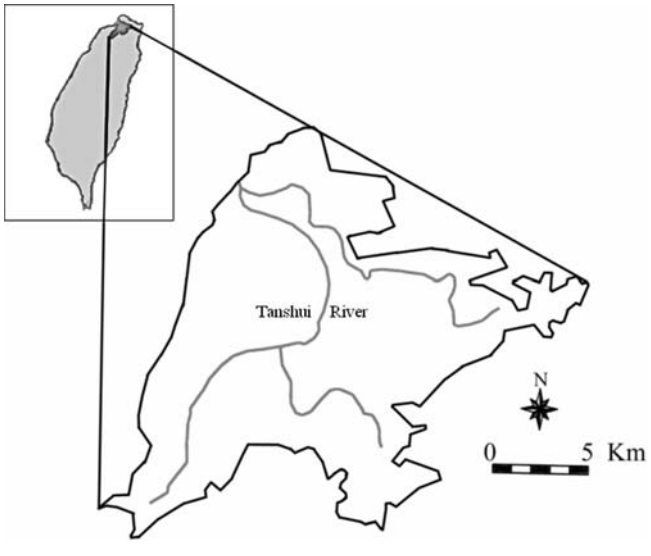

Fig. 3 The location of Taipei municipal basin

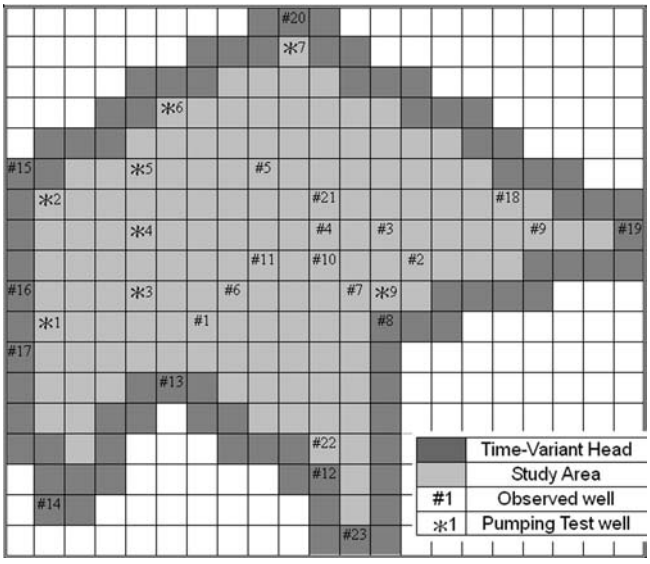

Fig. 4 The locations of hydraulic head observation wells and pumping test wells in the simulation area

Formulation of the optimal model

Refer to Eq. 5, the objective function can be defined and combined with the constraints to formulate the optimal model.

Table 1 The values of hydraulic conductivity *K* of ten drilling wells

Well	*K* (m/s)
*1	4×10^{-4}
*2	1×10^{-3}
*3	9×10^{-4}
*4	7×10^{-5}
*5	2×10^{-3}
*6	4×10^{-4}
*7	6×10^{-4}
*8	3×10^{-3}
*9	5×10^{-4}
*10	2×10^{-3}

$$\text{Min } Z = \left\{ \frac{1}{N_h \times T} \sum_{\mu=1}^{N_h} \sum_{t=1}^{T} \left(\frac{h_\mu(\Omega_n, t) - h_\mu^o(t)}{h_\mu^o(t)} \right)^2 + \lambda \frac{1}{N_k} \sum_{v=1}^{N_k} \left(\frac{K_v(\Omega_n) - K_v^{\text{prior}}}{K_v^{\text{prior}}} \right)^2 \right\}^{1/2} \tag{7a}$$

S.T.

$$T_s \frac{\partial^2 h}{\partial X^2} + T_s \frac{\partial^2 h}{\partial Y^2} = S \frac{\partial h}{\partial t}$$

$$T_s = K \times b,\ S = S_s \times b \tag{7b}$$

$$X_l \leqslant X_i \leqslant X_u, \quad i = 1, \ldots, n \tag{7c}$$

$$Y_l \leqslant Y_i \leqslant Y_u, \quad i = 1, \ldots, n \tag{7d}$$

$$\Omega_n = \text{VD}[V(P_i, k_i), \quad i = 1, \ldots, n] \tag{7e}$$

$$K_i = \alpha_i \times 10^{\beta_i} \quad i = 1, \ldots, n \tag{7f}$$

$$n = f(\text{PU}_n, \text{SE}_{n,n-1}) \tag{7g}$$

where N_h is the number of observed wells ($N_h = 9$, including #1,#3,#4,#5,#6,#7,#10,#11, and #21). The h_μ and h_μ^o are the simulated and observed hydraulic heads at time t. T_s is the transmissivity defined as the product of the horizontal conductivity K and the known thickness b of the confined aquifer. S is the storage coefficient defined as the product of the specific storage Ss and the known thickness b of the confined aquifer. In Eqs. 7c and 7d, the terms X_l. X_u, Y_l, and Y_u are given lower and upper bounds of the generator point coordinates. In the study, X_l and Y_l are set to 1 and X_u and Y_u are set to 21 and 18, respectively. The location (X_i, Y_i) of generator point P_i is decision variables. The step of the generator point movement is two grids ($\Delta X = 2$, $\Delta Y = 2$). The hydraulic conductivity K_i is also a decision variable, and decomposed as Eq. 7f to speed the searching process by determining α_i and β_i. Thus, the decision variables of this optimization problem can be defined as $\{X_i, Y_i, \alpha_i, \beta_i, i = 1,..., n\}$. Moreover, the optimized number (n) of zones is constrained by the parameter uncertainty (PU_n) and the structure error ($\text{SE}_{n,n-1}$) as Eq. 7g.

Specification of SA

Before SA is applied to optimize the spatial distribution of K, the cooling schedule must be given. According to Kirkpatrick et al. (1983), the number of iterations, L is set to be several times the number of decision variables $\{X_i, Y_i, \alpha_i, \beta_i, i = 1,...,n\}$. The starting temperature (τ_i) yields an initial 80% acceptable probability to move at least and is set to be 1. The value of 0.8 is assigned to the decrement of temperature. The ending temperature (τ_e) is set to be 0.01 to give a last 95% refused moving probability at least to ensure the convergence of the optimization.

Results and discussions

The proposed optimal procedure is applied to the Chingmei Layer to identify the optimal parameter structure. During the optimal procedure, the heads data observed in the year of 2000 are used for evaluating the RE, the PU and the observation space of SE, and those in 2001 are used for evaluating the prediction space of SE. Otherwise, the prior information of K-values is used for evaluating the parameter space of SE. Then, the optimal structure is determined by three criteria, the RE, the PU, and the SE.

The results of the optimal procedure are summarized in Tables 2 and 3. Figure 5 illustrates the RE, PU and SE with different numbers of zones, respectively. Fig. 5a shows that RE becomes flat after four zones. Meanwhile, whether the known data are sufficient to afford a higher parameter dimension should be considered. Thus, the PU and SE are further discussed based on Fig. 5b, c.

Figure 5b indicates there are two turning points with obviously increasing slopes after three zones and five zones. However, the slope after five zones is steeper than after three zones. Furthermore, the improvement of RE from three zones to four zones is significant. As a result, the suggesting parameter dimension determined by PU is the optimal structure with five zones.

The structure error is also discussed for the determination of parameter dimension. In Fig. 5c, the trend of $\text{SE}_{n,n-1}$ is decreasing. Referred to three kinds of spaces separately, the $d_{n,n-1}^{\text{obs}}$ is oscillated. Tsai et al. (2003b) suggested a stopping criterion that if $d_{n,n-1}^{\text{obs}}$ is smaller than 2η, which η is the head observation error, the $n-1$ zones is enough and adequate. However, there are only d_{32}^{obs} and d_{54}^{obs} smaller than 2η where η is 0.05. Although both d_{32}^{obs} and d_{54}^{obs} conformed to the suggested stopping criterion, d_{54}^{obs} is more appropriate to be applied to determine the optimal structure. Because considering the improvement of RE from three zones to four zones is significant, the parameter dimension should be

Table 2 Results summary for the Taipei Basin

	Two Zones	Three Zones	Four Zones	Five Zones	Six Zones
K1 (m/s)	4×10^{-3}	4×10^{-3}	4×10^{-3}	4×10^{-3}	4×10^{-3}
K2 (m/s)	8×10^{-5}	4×10^{-5}	8×10^{-5}	8×10^{-5}	8×10^{-5}
K3 (m/s)	–	8×10^{-4}	8×10^{-4}	8×10^{-4}	6×10^{-4}
K4 (m/s)	–	–	2×10^{-4}	6×10^{-4}	4×10^{-4}
K5 (m/s)	–	–	–	6×10^{-5}	4×10^{-4}
K6 (m/s)	–	–	–	–	2×10^{-4}
RE	0.143	0.129	0.105	0.099	0.098
PU ($\times10^6$)	0.075	0.431	1.567	1.860	3.190

Table 3 Structure errors between different optimal structures

Structure	Observation space, $d^{obs}_{n,n-1}$	Parameter space, $d^{par}_{n,n-1}$	Prediction space, $d^{pre}_{n,n-1}$	$SE_{n,n\text{-}1}$ ($\omega_1 = 1$, $\omega_2 = 0.1$)
2∼3	0.071	1.520	0.137	1.604
3∼4	0.167	1.360	0.276	1.554
4∼5	0.094	0.977	0.145	1.086
5∼6	0.192	0.360	0.392	0.591

increased. Here, the optimal structure with five zones is recommended.

Figure 5c shows that the trend of $d^{\text{par}}_{n,n-1}$ is decreasing with increasing the number of zones and d^{pre}_{54} is smaller than d^{pre}_{65} and similar to d^{pre}_{32}. As a result, the optimal structure with five zones is the most appropriate. From the analyses of three kinds of spaces, the conjunction of these results is the optimal structure with five zones. Thus, the conclusion of SE is also the same with the conclusion of PU.

Figure 6 illustrates the parameter structure of K in two, three, four, and five zones, respectively. From these figures, it can be shown that the similarity increases with adding the number of zones. Figure 7 illustrates the simulated and observed hydraulic heads of the observation space and the prediction space at the observation well#4. The hydraulic heads simulated by the optimal structure with five zones are approximate to the observed ones in both observation and prediction spaces.

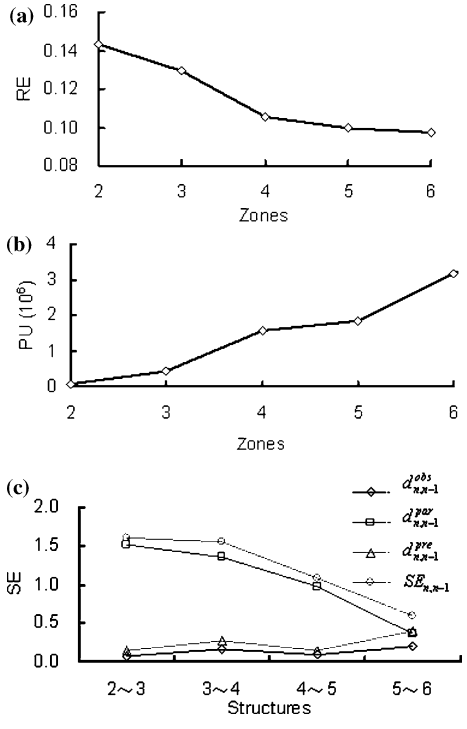

Fig. 5 **a** residual errors, **b** parameter uncertainty, and **c** structure errors resulting from different number of zones

Comparison with hill-climbing method

Tung et al. (2003) has proved that the zonation method with SA searching algorithm is better than MODFLOW built in inverse solver which using the Gauss–Marquardt–Levenberg method. In this study, the traditional hill-climbing (gradient) method is used to substitute SA to optimize the spatial distribution of hydraulic conductivity for further comparison. The hill-climbing method improves alternatives from current solution to its better neighbor solution. When there is no better neighbor solution, the searching process stops. Thus, the hill-climbing method tends to find a local optimal solution.

Table 4 shows residual errors of initial solution and optimal solutions identified by SA and the hill-climbing method, respectively. SA and the hill-climbing method have the same initial solution. According to Table 4, when the number of zone increases, residual errors are reduced for both SA and hill-climbing method. However, the SA always results in smaller residual error for different zonation patterns. The hill-climbing method is a local searching method and thus tends to find the local optimal. SA has the ability to escape from the local optimums and increase the probability to reach the global optimum, and thus has better results.

Conclusions and suggestions

The optimal procedure proposed in this study integrates VD with SA to optimize the spatial distribution of hydraulic conductivity and is applied to the Chingmei Layer, a confined aquifer. With three criteria, the optimal parameter structure of the groundwater model is identified successfully. The optimal structure with five zones provides reasonable hydraulic head simulation and even the prediction. It can be expected that the more prior information and observed data can result in more robust optimal parameter structure by using this optimal procedure.

The zonation method, VD, has been proved to be able to capture the spatial distribution of K effectively for the groundwater model in this case study. Furthermore, there are some advanced VDs, such as multiplicatively weighted VD, and additively weighted VD (Okabe et al. 1992), may be integrated to strengthen the proposed procedure in the future. For example, the

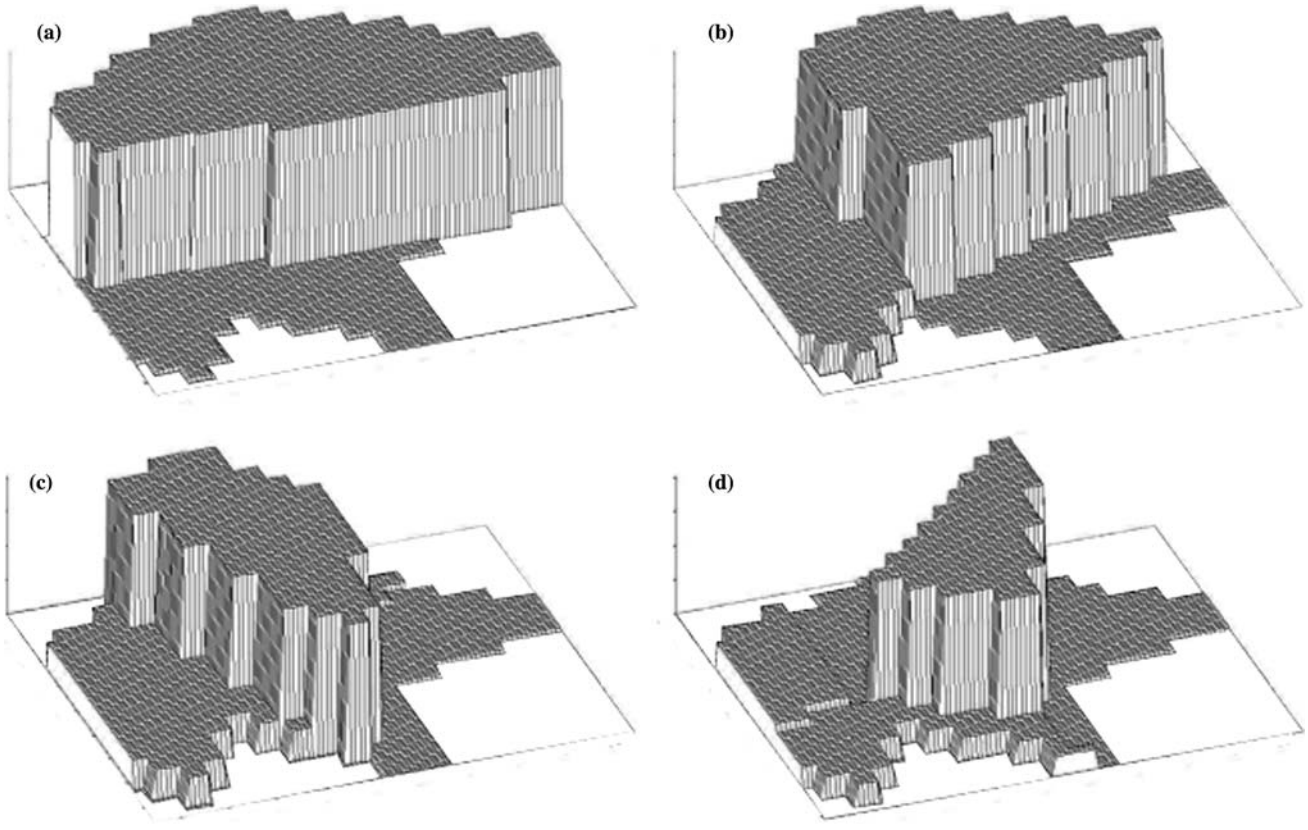

Fig. 6 The optimal structure with **a** two zones, **b** three zones, **c** four zones, **d** five zones

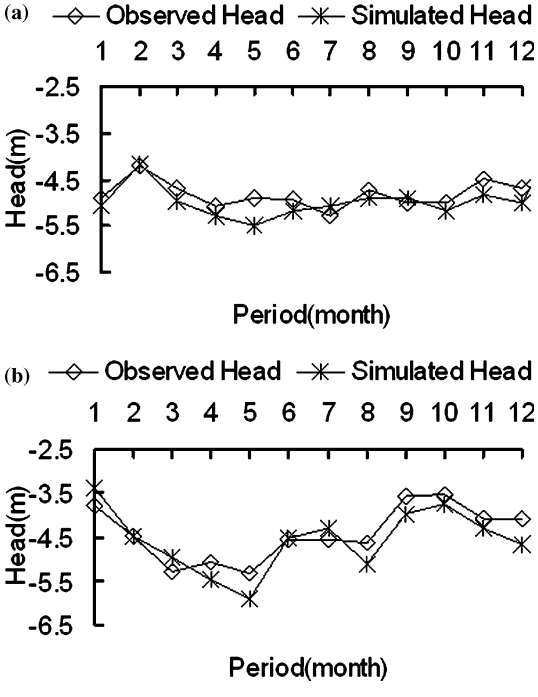

Fig. 7 Simulated and observed heads with five zones in the observation well#4 **a** observation space, **b** prediction space

anisotropic and even sinuous patterns can be depicted by the refined and robust VDs. Tung and Chou (2004) also applied different zonation methods to depict the spatial distribution of parameter.

The spatial distribution of K can be optimized efficiently by SA with finite searching iterations. However, when the parameter dimension increases, the feasible solution space will extend enormously. Thus, a refined cooling schedule of SA may be required in the further study. Other heuristic algorithms, such as tabu search and genetic algorithm, may also be able to play the role of SA to find optimal structure. However, which algorithm is more efficient is not discussed in this study and requires further study.

Table 4 The comparisons of residual errors between SA and Hill-climbing method

	The number of zones				
	Two	Three	Four	Five	Six
Initial solution	0.236	0.332	0.349	0.363	0.186
Hill-climbing	0.231	0.184	0.181	0.179	0.178
SA	0.143	0.129	0.105	0.099	0.098

Appendix

Covariance matrix for parameter uncertainty

A covariance matrix as given by Yeh and Yoon (1981) is used quantify the parameter uncertainty. The equation is listed as follows:

$$\mathrm{Cov}_n = \frac{1}{N_h \times T - n} \sum_{\mu=1}^{N_h} \sum_{t=1}^{T} \left(\frac{h_\mu(\Omega_n^*, t) - h_\mu^o(t)}{h_\mu(\Omega_n^*, t)} \right)^2 \left[J^{\mathrm{T}} J \right]^{-1}$$

where J is the Jacobian matrix of hydraulic head with respect to K.

Structure error

The three components of structure error are calculated as follows:

$$d_{n,n-1}^{\mathrm{obs}} = \sum_{g=1}^{N_g} \sum_{t=1}^{T} \left| \frac{h_g(\Omega_n^*, t) - h_g(\Omega_{n-1}^*, t)}{h_g(\Omega_n^*, t)} \right|$$

$$d_{n,n-1}^{\mathrm{par}} = \sum_{g=1}^{N_g} \left| \frac{K_g(\Omega_n^*) - K_g(\Omega_{n-1}^*)}{K_g(\Omega_n^*)} \right|$$

$$d_{n,n-1}^{\mathrm{pre}} = \sum_{g=1}^{N_g} \sum_{t=1}^{T} \left| \frac{h_g(\Omega_n^*, t) - h_g(\Omega_{n-1}^*, t)}{h_g(\Omega_n^*, t)} \right|$$

where N_g is the number of grids and T is the simulation or prediction periods.

References

Aarts EHL, Van Laarhoven PJM (1985) Statistical cooling: A general approach to combinatorial optimization problems. Philips J Res 40:193–226

Abdulla FA, Al-Khatib MA, Al-Ghazzawi ZD (2000) Development of groundwater modeling for the AZROQ basin. Environ Geol 40(1/2):11–18

Dirchlet GL (1850) Uber die Reduction der Positeven quadratischen Formen mit drei unbestimmten ganzen Zahlen. Journal of fur die Reine und Angewandte Mathematik 40:209–227

Dougherty DE, Marryott RA (1991) Optimal groundwater management 1. simulated annealing. Water Resour Res 27(10):2493–2508

Hsu RT (1985) Application of parameter identification on groundwater pumpage inverse problem. MS Thesis Graduate Institute of Agricultural Engineering National Taiwan University

Kirkpatrick S (1984) Optimization by simulated annealing: quantitative studies. J Stat Phys 34(5/6):975–986

Kirkpatrick S, Gelatt CD, Vecchi MP (1983) Optimization by simulated annealing. Science 220:671–680

Lin YP, Tan YC, Rouhani S (2001) Identifying spatial characteristics of transmissivity using simulated annealing and kriging methods. Environ Geol 41:200–208

Metropolis N, Rosenbluth A, Rosenbluth M, Teller A, Teller E, Chem J (1953) Equation of state calculations by fast computation machines. Phys 21:1087–1092

Okabe A, Boots B, Sugihara K (1992) Spatial tessellations: concepts and applications of Voronoi Diagrams, 1st edn. John Wiley & Sons, Chichester

Sophocleous MA, Koelliker JK, Govindaraju RS, Birdie T, Ramireddygari SR, Perkins SP (1999) Integrated numerical modeling for basin-wide water management: the case of the Rattlesnake Creek basin in south-central Kansas. J Hydrol 214: 179–196

Sun NZ, Yang SL, Yeh WWG (1998) A proposed stepwise regression method for model structure identification. Water Resour Res 34(10):2561–2572

Thiessen AH (1911) Precipitation averages for large areas. Monthly Weather Rev 39:1082–1084

Tsai FTC, Sun NZ, Yeh WWG (2003a) Global-local optimization for parameter structure identification in three-dimensional groundwater modeling. Water Resour Res 39(2):1043–1056

Tsai FTC, Sun NZ, Yeh WWG (2003b) A Combinatorial optimization scheme for parameter structure identification in ground water modeling. Ground Water 41(2):156–169

Tung CP, Chou CA (2002) Application of tabu search to groundwater parameter zonation. J Am Water Resour Assoc 38(4):1115–1126

Tung CP, Chou CA (2004) Pattern classification using tabu search to identify the spatial distribution of groundwater pumping. Hydrogeol J 12:488–496

Tung CP, Tan CC, Lin YP (2003) Improving groundwater flow modeling using optimal zoning methods. Environ Geol 44:627–638

Voronoi G (1908) Nouvelles applications des parameters continues a la theorie des formes quadratiques. Deuxieme Memoire: Recherches sur les parallelloedres primitives. Journal fur die Reine und Angewandte Mathematik 134:198–287

Yeh WWG (1986) Review of parameter identification procedures in groundwater hydrology: The inverse problem. Water Resour Res 22(2):95–108

Yeh WWG, Yoon YS (1981) Aquifer parameter identification with optimum dimension in parameterization. Water Resour Res 17(3):664–672

Yeh WWG, Yoon YS, Lee KS (1983) Aquifer parameter identification with kriging and optimum parameterization. Water Resour Res 19(1):225–233

Zheng C, Wang P (1996) Parameter structure identification using tabu search and simulated annealing. Adv in Water Resour 19(4):215–224